From Diesel to Electric: Exploring Fleet Increment Curves for Zero-Emission Bus Transition

Yiyang Peng, Zhuowei Wang, and Anthony Chen

***Abstract*—Bus electrification is a key trend in the global evolution of public transportation systems. However, replacing diesel buses (DBs) with Battery electric buses (BEBs) is a long-term process, where the limited driving range and prolonged charging times might necessitate a larger BEB fleet to maintain trip services compared to the replaced DB fleet. To quantify this fleet expansion across variable replacement decisions, we introduce the fleet increment curve (FIC), a novel conceptual idea that guides BEB procurement decisions during the transition to the zero-emission bus (ZEB) system. First, the FIC is derived from solving a series of mixed-integer linear programming (MILP) (namely MILP-FIC model) by varying the replaced DB fleet as inputs, where each MILP is developed by means of linearization techniques, while formulating the mixed-fleet operation under limited charging accessibility. To solve the MILP-FIC, Lagrangian relaxation (LR) is applied to relax charging accessibility constraints, decomposing the problem into route-specific subproblems. Subsequently, representing FIC by-products as piecewise linear functions enables extended models developed for addressing long-term fleet replacement scheduling and charging resource allocation. A general fleet replacement scheduling is presented, which accommodates multiple BEB types (varying battery capacities and charging power) by deriving type-specific fleet procurement curves. We use real-world bus route data from Hong Kong to explore the FIC, revealing how route characteristics—such as trip frequency, trip duration, and energy consumption—interact with charging site characteristics (e.g., siting and sizing) to shape the FIC. The curves typically follow a non-decreasing trend, while an S-shaped trend occurs across certain routes. Additionally, the results demonstrate the effective incorporation of FIC into the planning for ZEB transition, providing valuable insights for bus operators.**

***Index Terms*—Zero-emission bus transition, fleet increment curve, charging accessibility, mixed-integer linear program, Lagrangian relaxation.**

I. Introduction

A. Background

THE zero-emission bus (ZEB) transition from diesel to electric has become a global priority for achieving carbon neutrality in public transit, driven by the urgent need to mitigate climate change and reduce greenhouse gas emissions. Battery electric buses (BEBs) are now the primary technology adopted for fleet decarbonization, with many cities and countries setting ambitious electrification targets. By 2024, there are over 70,000 BEBs worldwide, with China accounting for 70% and the remainder primarily in Europe (notably the United Kingdom (U.K.), Italy, Germany, Denmark, Finland, the Netherlands, and Norway), the United States (U.S.), and India [1]. However, this transition from diesel buses (DBs) to BEBs is not a one-shot process; rather, it is a complex, long-term undertaking that often spans years. For example, Shenzhen (China) began electrifying its bus fleet in 2009 and achieved full electrification by 2017, operating 6,053 EBs [2]. Cities like Hong Kong face greater challenges due to their heavy reliance on buses in public transport, prevalence of double-decker buses, and limited space for parking buses and deploying charging infrastructures. These restrictions make fleet replacement management more challenging to maintain trip service levels, particularly during the ZEB transition. Moreover, the extended timeline necessitates the operation of mixed fleets—comprising both traditional DBs and EBs—during the transition, which introduces significant operational and strategic challenges for bus operators.

B. Motivation

When using the same type of vehicle to replace the original one, the fleet size usually remains the same to keep the current trip service. However, unlike this 1:1 bus fleet replacement (BFR), replacing DBs with EBs requires 1:X BFR, where X is sometimes a number larger than 1, arising from the operational limitations of EBs relative to DBs, notably shorter driving ranges and longer charging times. In cases where the BEB driving range meets or exceeds daily mileage requirements, overnight charging is sufficient, and a 1:1 BFR may suffice [3]–[5]. By contrast, when BEBs sometimes cannot meet daily mileage demands, additional daytime charging is required. In Hong Kong, for instance, even the latest battery and charging technology requires BEBs to charge for approximately two hours [6]. Compounding this, the city's space constraints make it difficult to install sufficient charging infrastructure at every bus terminal. Given the longer charging duration and suboptimal charging resource allocation (e.g., insufficient chargers and distant detour charging), a 1:1 BFR may be inadequate to maintain trip service levels. As a result, the dissatisfaction with daily mileage requirements prompts operators to consider fleet expansion during the ZEB transition. In this study, we introduce a 2-dimensional *Fleet Increment Curve (FIC)* to highlight this fleet expansion, while ensuring compliance with operational feasibility (trip service constraints and limited charging accessibility). Figure 1 illustrates a possible FIC configuration. For a BFR of 1:X, X may be greater than 1

The work described in this paper was jointly supported by the Project of Strategic Importance (1-ZE0A) and the Research Institute of Sustainable Urban Development (1-BBG1 and 1-BBWW) at the Hong Kong Polytechnic University, Hong Kong. (Corresponding author: Anthony Chen).

Yiyang Peng, Zhuowei Wang, and Anthony Chen are with Department of Civil and Environmental Engineering, The Hong Kong Polytechnic University, Kowloon 100872, Hong Kong SAR (e-mail: yiyang.peng@connect.polyu.hk; zhuowei.wang@connect.polyu.hk; anthony.chen@polyu.edu.hk).

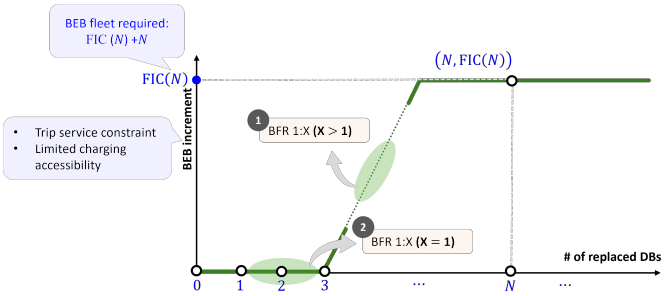

Fig. 1. A possible FIC illustrating the relationship between BEB increment and the BFR.

(Type 1) or equal to 1 (Type 2) with different DB replacement decisions. Type 1 BFR reflects a positive BEB increment when replacing more than 3 DBs, while Type 2 BFR signifies no expansion for BEB fleet if the replaced DB fleet is no larger than 3 for this example.

Let FIC represent a general function, for a given number of DBs to be replaced (N in Figure 1), the corresponding BEB fleet increment is obtained as FIC(N). Accordingly, the total number of BEBs to be procured equals FIC(N) + N. As shown in Figure 1, the point placement rule over the FIC is as follows: with a given replaced DB fleet, find the minimum BEB increment to maintain trip services while adhering to existing charging allocation. Using this information from FIC, bus operators can optimize fleet replacement scheduling to enhance asset management efficiency. Additionally, the fleet increment projections derived from the FIC offer valuable insights for infrastructure planning, such as depot expansions for bus parking and the deployment of charging facilities to support the ZEB system.

II. Literature Review and Contributions

A. Related studies

The ZEB transition requires a long-term decision that relies on the economic (e.g., investment, lifecycle costs, and operational expense) and environmental objectives. Specifically for economic objectives, Li et al. [3] a case study in Hong Kong specifically accounted for the remaining life additional benefit of existing DBs. Pelletier et al. [7] examined the implications of different charger types (e.g., slow and fast plug-in, wireless) and charging locations (depot, terminal, bus stop). Environmental objectives are also prominent, given the overarching goal of carbon neutrality, though the specific metrics and impacts assessed vary by context. For instance, Ye et al. [5] conducted comparative analyses of EB replacement planning in London, Toronto, and Philadelphia, focusing on air and water pollutant emissions. Operational expenses have been widely incorporated into determining fleet replacement strategies. Islam and Lownes [4] predefined time-variant operational costs per mile for different bus types. Navarrete et al. [8] applied the real-world operational data and involved it in calculating the total exploitation cost. Avenali et al. [9] simulated the time-variant EB fleet size and combined the given energy consumption to obtain the total operational expenses. Zhou et al., [10] optimally obtained decisions related to bus purchase, charger deployment, and bus salvage to satisfy the requirement of travel demand, budget, and charging demand. During the ZEB transition, catering to the existing bus network and charging infrastructure configuration is of paramount importance to efficiently integrate EBs [11], while the aforementioned studies paid less attention to satisfying operational constraints (whether the introduced BEB fleet ensures all trips are serviced with limited charging infrastructure) over the long-term ZEB transition.

In the public transit operation, addressing the vehicle scheduling problem (VSP) can optimally manage the fleet composition adhering to trip service constraints. The transition to the ZEB system involves managing a mixed fleet of DBs and EBs, requiring optimized VSP to determine an ideal fleet composition. Lu et al. [12] incorporated micro-level driving conditions to estimate trip times in their mixed-fleet VSP model development. Yıldırım and Yıldız [13] considered EBs with multiple battery sizes and charging technologies, and built a pricing graph for each bus type to find good feasible EB schedules through column generation. Cong et al. [14] developed a nonlinear model to formulate a collaborative vehicle-crew scheduling with a mixed fleet of electric and fuel buses. However, as ensuring operational feasibility of EBs also depends on the requirement of sufficient charging infrastructure, these studies overlooked the impact of the limited charging accessibility when scheduling EBs. Alvo et al. [15] developed a two-stage model to incorporate the limited charging accessibility, where the first stage generated EB schedules without charging constraints, then refined them via feasibility cuts derived from the second stage. Peng et al. [16] developed a mixed-integer linear programming (MILP) to address the mixed-fleet operation of BEBs and hydrogen buses, where the limited charging accessibility was formulated by incorporating waiting time and refueling amount variables. de Vos et al. [17] modeled state of charge (SOC) dynamics of EBs via a connection-based network, while tracking the remaining energy during the daily operation. Overall,

TABLE I
Summary of Studies Related to Fleet Determination for the ZEB Development

References	Operational constraints [1]		Long-term BFR decisions [2]
	Trip service	Limited charging	
[3]–[5], [7]–[10]	×	×	√
[12]–[14]	√	×	×
[15]–[17]	√	√	×
This study	√	√	√

[1] A fixed scheduling/fleet composition meeting trip service and charging constraints (without time-indexed variables).
[2] A strategic fleet replacement/acquisition decision made for a planning horizon (with time-indexed variables).

the aforementioned studies aimed to find an optimal fleet composition for cost efficiency (minimization of operational costs), while no focus on the fleet composition adaptive to a certain level of bus system electrification. Table I organizes the related works to fleet determination, according to their focus on either operational constraints or long-term decisions

for the ZEB development. Our study aims to ensure that the fleet replacement/acquisition decision over the planning horizon is operationally valid. Given a BFR decision over the ZEB transition, bus operators can periodically adjust the fleet scheduling and determine an optimal required BEB fleet.

To incorporate operational constraints into long-term decisions made in the electrified transport system, Shehabeldeen et al. [18] developed a multi-stage optimization model to optimize battery replacement schedules (considering battery degradation) in a ZEB transit system. This model enabled periodic adjustment of charging schedules alongside multi-stage charging infrastructure planning. The authors employed a surrogate model-based space mapping algorithm to address the nonlinearity of battery degradation rates. Cui et al. [19] provided a fleet replacement scheduling model during the zero-emission transition of electric ships, while highlighting that their work is different from existing studies that determined the fleet size without incorporating actual operational conditions into the planning horizon. In their developed mixed-integer nonlinear programming, more time-indexed variables (e.g., operation-related) are included to facilitate the joint optimization. However, this comprehensive model will significantly increase the scale of variables and constraints, making it intractable to obtain exact solutions. We avoid a complex integrated formulation by separating the problem into two linear models: one without time-indexed variables and one with time-indexed variables. The connection between them is established through the FIC. This methodology allows us to obtain exact, operationally feasible long-term BFR decisions.

B. Contributions and outline

To address the research gap revealed in Table I, this study is motivated by exploring the FIC of BEB fleet expansion when replacing the DB fleet. Deriving FIC explicitly incorporates critical operational constraints (trip service and limited charging), while it provides a foundation for optimizing long-term decisions like fleet replacement scheduling and charging resource allocation. The main contributions of this paper are summarized below:

- A MILP, namely the MILP-FIC model, is developed to obtain the minimum BEB fleet adaptive to a given replaced DB fleet, where the output BEB fleet should maintain trip services with the existing charging resource allocation.
- A Lagrangian Relaxation (LR) algorithm is employed to solve the MILP-FIC model, which can efficiently handle the charging constraints, resulting in several route-specific subproblems to be solved.
- FIC by-products, represented as piecewise linear functions, enable smooth incorporation into two practical planning models: fleet replacement scheduling (long-term decisions) and charging resource allocation3, where exact solutions can be obtained instead of solving an intractable integrated model.

The remainder of this paper is organized as follows. Section III preliminarily describes the MILP-FIC model and issues to be addressed. Section IV develops the MILP-FIC model to obtain FIC. Section V introduces the LR algorithm for solving the MILP-FIC model. Section VI provides two FIC-incorporated planning models over the ZEB transition. Section VII presents an extension to address the BFR decision of multiple BEB types over the ZEB transition. Section VIII shows numerical results of FIC and FIC-incorporated planning models, and Section IX concludes the paper.

III. Preliminary of the MILP-FIC model

As bus systems shift toward ZEB, determining the optimal number of BEBs to facilitate certain DB replacement decisions becomes crucial for operators. Since a 1:1 BFR may not be feasible due to the limited driving range and longer charging times of BEBs, the difference between the BEB purchasing fleet and the replaced DB fleet reflects the *BEB increment*. This study introduces the FIC to quantify the relationship between the replaced DB fleet and BEB increment. Herein, we analyze FICs for individual routes and output route-specific guidance. Let R collect all the bus routes, where N^r represents the DB fleet replaced on route $r \in R$. The FIC then acts as a mapping ($\text{FIC} : N^r \mapsto P^r - N^r$), where P^r denotes the optimal BEB fleet to replace N^r DBs on route r. Notably, when the total DB fleet to be replaced is M^r, a complete FIC involves different N^r ranging from 0 to M^r in 1-unit increments.

To fix the Y-axis value of FIC, deriving P^r for ensuring operational feasibility introduces the challenge of addressing trip service and charging constraints, with a detailed description provided in the following subsections.

The main assumptions are listed as follows:

- A1 The backup bus fleet is ignored for simplicity. Therefore, the entire bus fleet must actively serve trips.
- A2 The study explores route-specific FIC and does not account for deadheading between routes.
- A3 DBs are assumed to operate without energy replenishment or range restrictions.

A. Mixed-fleet vehicle scheduling

During the ZEB transition until DBs are 100% replaced, public transit operators must manage a mixed fleet of DBs and BEBs. To ensure the trip service constraint, vehicle scheduling is a key component to allocate the mixed fleet to serve compatible trip pairs.

For route $r \in R$, subset $\mathcal{T}^r$ collect trips of route r. Accordingly, the compatibility between trips can be graphically represented as route-specific networks shown in Figure 2 ($r_1, r_2 \in R$), where the source node (o)/sink node (d) is used to track the fleet utilization of each route. $\Omega^r = \{(o,i),(i,d)|\forall i \in \mathcal{T}^r\} \cup \{(i,j)|s_i + T^r \leq s_j|\forall i,j \in \mathcal{T}^r\}$ is used to collect all compatible trip pairs of route r, where s_i is the start time of trip i and T^r represents the round-trip duration of route r. Consequently, directed arcs can be generated between two trip service nodes in Figure 2, if the corresponding trip pair belongs to Ω^r.

For a mixed-fleet operation, DB and BEB act as two commodities along the black arcs of networks, using binary variables $x_{ij}^{r,\mathbf{d}}$ and $x_{ij}^{r,\mathbf{e}}$ to represent whether a trip pair $(i,j) \in \Omega^r$ is served by a DB or BEB, respectively. By

contrast, only BEB is involved for the arcs crossing charging events, shown as bold purple arrows in Figure 2.

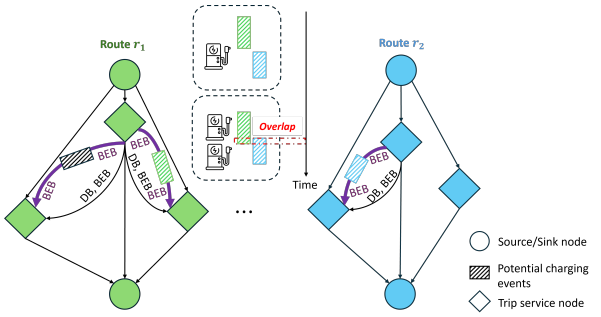

Fig. 2. Network flow representation for mixed-fleet operation addressing charging accessibility. The colored hatched square (green and blue for Route r_1 and Route r_2, respectively) indicates that these two charging events are conducted. Route r_1 and Route r_2 share the same charging site, where an additional charger is needed if two activated charging events overlap over the time horizon.

B. Limited charging accessibility

Due to the limited driving range of BEBs, opportunity charging during the daily operation is necessary to prevent BEBs from being disrupted, making them available for serving more trips and reducing the BEB fleet size. Section III-A obtains Ω^r that provides the potential charging opportunity for BEBs. In high-density urban areas, installing charging stations at every route terminal is impractical. Instead, a centralized charging site is preferred, though this requires BEBs to detour from terminals to the site. Here, all the routes in R share this centralized charging service, where BEBs should take additional energy and time for the detouring process. Let t^r represent the additional time for this detour of route $r \in R$. Consequently, for any compatible trip pair $(i,j) \in \Omega^r$, the potential charging duration is calculated as: $W^r_{ij} = s_j - s_i - T^r - 2t^r$. Since only BEBs need to consider charging events, binary variable z^r_{ij} is defined specifically for BEBs, indicating whether this potential charging event can be conducted, where charging decisions (z^r_{ij}) are tightly dependent on the BEB-trip allocation ($x^{r,\mathbf{e}}_{ij}$). Note that $z^r_{ij} = 0$ if $i = o$ or $j = d$, and two scenarios make it impossible to conduct potential charging events: $z^r_{ij} = 0$ if $W^r_{ij} < 0$ or $x^{r,\mathbf{e}}_{ij} = 0$.

The limited charging accessibility indicates that the number of charging events that are simultaneously served cannot exceed the number of chargers (denoted as C). Once potential charging events are conducted, see the two colored hatched squares (green and blue for Route r_1 and Route r_2) in Figure 2, these two activated charging events share a centralized charging site. Over a time horizon, two chargers are needed if their corresponding charging periods overlap. To enforce the constraint of limited charging accessibility, we discretize the operational timeline into a set of fine time slots Λ. For each slot $\lambda \in \Lambda$, the number of activated charging events that occupy this slot should not be larger than C.

IV. MILP-FIC MODEL

This section develops the MILP-FIC model to obtain the sampling points over the FIC. Given the exogenous N^r (X-axis value) ranging from 1 to M^r, the MILP-FIC formulation aims to find the optimal P^r for maintaining trip services utilizing the given charging resources, where the Y-axis value equals $P^r - N^r$. Table II lists the notations used in the MILP-FIC model.

TABLE II
LIST OF NOTATIONS USED IN THE MILP-FIC MODEL

Set	
R	Route set sharing a centralized charging site.
Ω^r	Compatible trip pair set of route $r \in R$.
$\mathcal{T}^r$	Trip set of route $r \in R$.
Λ	Set of time slots.
Parameters	
C	Number of available chargers.
s_i	Start time of trip $i \in \mathcal{T}^r$.
E^r	Round-trip energy use of route $r \in R$.
T^r	Round-trip time use of route $r \in R$.
W^r_{ij}	Potential charging duration within trip pair $(i,j) \in \Omega^r$.
e^r	Energy use between the terminal of route $r \in R$ and the charging site.
t^r	Time use between the terminal of route $r \in R$ and the charging site.
$\overline{e}^r$	Energy use between the terminal of route $r \in R$ and the depot.
D	BEB battery capacity.
$\delta^{r,\lambda}_{ij}$	If time slot λ is occupied by the charging event within trip pair $(i,j) \in \Omega^r$, $\delta^{r,\lambda}_{ij} = 1$. Otherwise, $\delta^{r,\lambda}_{ij} = 0$.
N^r	Number of DBs to be replaced on route r
M^r	Number of DBs before the ZEB transition for route r, where $N^r = 0$.
Intermediate variables	
Q^r_i	BEB remaining energy after completing trip $i \in \mathcal{T}^r$.
$\overline{Q}^r_i$	BEB remaining energy after completing the previous trip of trip $i \in \mathcal{T}^r$.
Decision variables	
$x^{r,v}_{ij}$	If trip pair $(i,j) \in \Omega^r$ is served by the same bus of type v, $x^{r,v}_{ij} = 1$. Otherwise, $x^{r,v}_{ij} = 0$.
z^r_{ij}	If a BEB charges during W^r_{ij}, $z^r_{ij} = 1$. Otherwise, $z^r_{ij} = 0$.

During the ZEB transition, minimizing the acquisition BEB fleet is paramount. Therefore, the objective of the MILP-FIC model is formulated as:

$$\min_{x^{r,v}_{ij}, z^r_{ij} \in \{0,1\}} \mathcal{Z} = \sum_{r \in R} \sum_{i:(o,i) \in \Omega^r} x^r_{oi}, \tag{1}$$

where DBs and BEBs are indexed by $\mathbf{e}$ and $\mathbf{d}$, respectively. The constraints of the MILP-FIC model are classified as flow-related constraints, energy-management constraints, DB-replacement constraint, and charging-accessibility constraint.

Flow-related constraints:

$$\sum_{j:(i,j) \in \Omega^r} x^{r,v}_{ij} = \sum_{j:(j,i) \in \Omega} x^{r,v}_{ji} \quad \forall v \in \{\mathbf{e}, \mathbf{d}\} \ \forall r \in R \ \forall i \in \mathcal{T}_r, \tag{2}$$

$$\sum_{v} \sum_{j:(i,j) \in \Omega^r} x^{r,v}_{ij} = 1 \quad \forall r \in R \ \forall i \in \mathcal{T}_r, \tag{3}$$

$$x^r_{ij} \geq z^r_{ij} \quad \forall r \in R \ \forall (i,j) \in \Omega^r, \tag{4}$$

$$W^r_{ij} z^r_{ij} \geq 0 \quad \forall r \in R \ \forall (i,j) \in \Omega^r. \tag{5}$$

Constraint (2) indicates the flow conservation for bus type v that serves trip i of route r. Constraint (3) stipulates that all the trips should be served, and each trip should be served by a single bus. Constraint (4) is a logical constraint, where the BEB charging can be activated (i.e., $z_{ij}^r = 1$) only if this BEB serves trip pair (i, j). Constraint (5) implies that BEB charging is impossible if the potential charging duration is less than 0.

Energy-management constraints:

$$Q_o^r = D - \overline{e}^r \quad \forall r \in R, \tag{6}$$

$$\overline{Q}_i^r = \sum_{j:(j,i)\in\Omega^r} x_{ji}^{r,\mathbf{e}} Q_j^r \quad \forall r \in R\ \forall i \in \mathcal{T}^r, \tag{7}$$

$$Q_i^r = (1 - \sum_{j:(j,i)\in\Omega^r} z_{ji}^r)\overline{Q}_i^r + \sum_{j:(j,i)\in\Omega^r} z_{ji}^r \left(\Phi\left(\Phi^{-1}\left(\overline{Q}_i^r - e^r\right) + W_{ji}^r\right) - e^r\right) - \sum_{j:(j,i)\in\Omega^r} x_{ji}^{r,\mathbf{e}} E^r \quad \forall r \in R\ \forall i \in \mathcal{T}^r, \tag{8}$$

$$\sum_{j:(i,j)\in\Omega^r} x_{ij}^{r,\mathbf{e}}(Q_i^{r,u} - e^r - 0.2D) \geq 0 \quad \forall r \in R\ \forall i \in \mathcal{T}_r, \tag{9}$$

$$\sum_{j:(i,j)\in\Omega^r} x_{ij}^{r,\mathbf{e}}\left(Q_i^{r,u} - (D - E^r - e^r)\right) \leq 0 \quad \forall r \in R\ \forall i \in \mathcal{T}_r. \tag{10}$$

In detail, Constraint (6) provides the remaining energy when a BEB is initially pulled out from the depot (fully charged) and arrives at the terminal of route r. Constraints (7) and (8) calculate the remaining energy after finishing the previous trip of trip $i \in \mathcal{T}^r$ and after completing trip $i \in \mathcal{T}^r$, respectively. When tracking the remaining energy of BEBs, Q_i^r should be bounded for trip $i \in \mathcal{T}_r$ served by BEBs if $\sum_{j:(i,j)\in\Omega^r} x_{ij}^{r,\mathbf{e}} = 1$. More specifically, Constraints (9) and (10) provide the lower bound and upper bound of remaining energy, respectively. Note that Constraints (7)-(10) consist of nonlinear terms (e.g., $x_{ij}^{r,\mathbf{e}} Q_i^r$). However, this format with the multiplication of binary variables and continuous variables can be efficiently linearized using the big-M method. The function Φ^u follows a nonlinear charging profile, which can be approximated as a piecewise linear function [20]. To approximate the The detailed linearization techniques can be found in [21].

Remark 1: Constraint (9) ensures that a BEB after serving trips has sufficient remaining energy to arrive at the charging site, while avoiding falling below the lowest allowance SOC that is usually set as 20%. Constraint (10) states that $Q_i^r \leq D - E^r - e^r$ if trip i is served by EB. Suppose that a BEB gets charged before serving trip i, the remaining energy ($\overline{q}$) after charging should satisfy $\overline{q} \leq D$ due to the battery capacity. As a result, $Q_i^r = \overline{q} - e^r - E^r \leq D - e^r - E^r$ to ensure that BEBs cannot experience a long charging duration to replenish them beyond the battery capacity. In other words, this constraint enforces that the duration of the selected charging event is 100% used. Indeed, Constraints (9) and (10) can be reformulated as:

$$Q_i^r/(D - E^r - e^r) \leq x_{ij}^{r,\mathbf{e}} \leq Q_i^r/(e^r + 0.2D)$$

As the conducted charging events are endogenously determined, it is possible that $\Phi^{-1}\left(\overline{Q}_i^r - e^r\right) + W_{ji}^r$ exceeds the upper limit of function Φ over charging duration. For instance, suppose the maximum charging duration is 2 hours (from zero remaining energy to full energy), where the detailed nonlinear charging profile is provided in Section VIII. To avoid further adding of breaking points, the slope of the final interval is carried on with a larger upper limit. Then, the implementation of Constraint (10) can ensure that the charging events whose $\Phi^{-1}\left(\overline{Q}_i^r - e^r\right) + W_{ij}^r$ exceeds 2 hours will not be selected.

DB-replacement constraint:

$$\sum_{i:(o,i)\in\Omega^r} x_{oi}^{r,\mathbf{d}} = M^r - N^r \quad \forall r \in R. \tag{11}$$

Constraint (11) states that N^r DBs are replaced, and the remaining DB fleet in operation should be $M^r - N^r$, where M^r is the fleet size before ZEB transition. Here, M^r is obtained by only optimizing $x_{ij}^{r,\mathbf{d}}$ while considering Constraints (2) and (3), whose objective is to minimize the total DB fleet size.

Charging-accessibility constraint:

$$\sum_r \sum_{(i,j)\in\Omega^r} z_{ij}^r \delta_{ij}^{r,\lambda} \leq C \quad \forall \lambda \in \Lambda, \tag{12}$$

Remark 1 implies that the duration of all selected charging events is 100% utilized. $\delta_{ij}^{r,\lambda}$ is an occupancy indicator of time slot λ. $\delta_{ij}^{r,\lambda} = 1$ if the period of time slot λ is within $s_i + T^r + t^r \sim s_j - t^r$. When C chargers are deployed at the centralized charging site, the number of served charging events sharing any sufficiently small time slot cannot exceed C.

Solving the MILP-FIC model: (1)-(12), $P^r = \mathcal{Z}^{r*} = \sum_{i:(o,i)\in\Omega^r} \overline{x}_{oi}^{r,\mathbf{e}}$, where $\overline{x}_{oi}^{r,\mathbf{e}}$ denotes the optimal solution. The FIC can be obtained with different replacement decisions (N^r) and their corresponding values of $P^r - N^r$. Additionally, $\mathcal{Z}^* = \sum_r P^r$ by aggregating the P^r of all routes.

V. Solving approach

This section presents the Lagrangian relaxation (LR) approach for efficiently solving the MILP-FIC model. Let μ_λ be the Lagrangian multiplier to penalize the violation of Constraint (12). The objective after LR is:

$$\min_{x_{ij}^{r,v}, z_{ij}^r} \mathcal{Z} + \sum_{\lambda\in\Lambda} \mu_\lambda \left(\sum_r \sum_{(i,j)\in\Omega^r} z_{ij}^r \delta_{ij}^{r,\lambda} - C\right). \tag{13}$$

As $\sum_{\lambda\in\Lambda} \mu_\lambda C$ is a constant, the objective can be simplified as:

$$\min_{x_{ij}^{r,v}, z_{ij}^r} \mathcal{L}(\boldsymbol{\mu}) = \mathcal{Z} + \sum_{\lambda\in\Lambda} \mu_\lambda \left(\sum_r \sum_{(i,j)\in\Omega^r} z_{ij}^r \delta_{ij}^{r,\lambda}\right). \tag{14}$$

Consequently, the model after LR can be solved with the following subproblems upon the decomposition of routes.

$$\min_{x_{ij}^{r,v}, z_{ij}^r} \mathcal{L}^r(\boldsymbol{\mu}) \quad \text{s.t.} (2) - (11). \tag{15}$$

The route-based subproblem is solved with given μ, which is updated over iterations. The update strategy for μ at iteration $k+1$ is:

$$g_\lambda^{(k)} = \sum_r \sum_{(i,j)\in\Omega^r} z_{ij}^{r(k)} \delta_{ij}^{r,\lambda} - C \quad \forall \lambda \in \Lambda, \tag{16}$$

$$\mu_\lambda^{(k+1)} = \max\left(0, \mu_\lambda^{(k)} + \alpha^{(k)} g_\lambda^{(k)}\right) \quad \forall \lambda \in \Lambda. \tag{17}$$

The Pseudo-code of the LR is given in Algorithm 1, and $\alpha^{(k)} = \left(UB - LB^{(k)}\right) / \sum_\lambda {g_\lambda^{(k)}}^2$. Here, $\overline{\mathbf{x}}$ is denoted to collect the feasible optimal solution of $x_{ij}^{r,\mathbf{e}}$. $\mathbf{x}^r$ and $\mathbf{z}^r$ are solution collection after solving the subproblem of specific route $r \in R$.

When existing time slots do not satisfy the charging accessibility constraint (12), a REPAIRINFEASIBLE function can be used to find feasible solutions. In detail, we find trip pair (i,j) whose z_{ij}^r equals 1 from $\mathbf{z}^{r*}$ and calculate their related value of $\sum_\lambda \mu_\lambda \delta_{ij}^{r,\lambda}$, while sorting this value in a decreasing order. After that, we use a greedy strategy to sequentially enforce $z_{ij}^r = 0$ according to the decreasing order. By adding this constraint, the feasible solution is found by solving the subproblems until Constraint (12) for any time slot in Λ can be satisfied. Note that REPAIRINFEASIBLE is used to speed up the update of UB, while it can be removed as the violation of Constraint (12) can lead to the update of μ_λ.

Algorithm 1 Pseudo-code of the LR

$k \leftarrow 0, LB \leftarrow -\infty, UB \leftarrow +\infty, \mu_\lambda \leftarrow 0\ \forall\lambda$.
while $k \le max\_iter$ and $gap \ge \epsilon$ **do**
  $\mathcal{L} \leftarrow 0$
  for $r \in R$ **do**
    $\mathcal{L}^{r*}, \mathbf{x}^{r*}, \mathbf{z}^{r*} \leftarrow$ SOLVESUBPROBLEM($\mu^{(k)}$)
    $\mathcal{L} \leftarrow \mathcal{L} + \mathcal{L}^{r*}$
  end for
  $LB^{(k)} \leftarrow \mathcal{L} - \sum_{\lambda\in\Lambda} \mu_\lambda C$
  $LB \leftarrow \max\left(LB, LB^{(k)}\right)$
  if $\exists\lambda$ violates Constraint (12) **then**
    $\overline{\mathbf{x}} \leftarrow$ REPAIRINFEASIBLE($\mathbf{x}^{r*}, \mathbf{z}^{r*}$)
  else
    $\overline{\mathbf{x}} \leftarrow \mathbf{x}^{r*}, \forall r$
  end if
  $\mathcal{Z} \leftarrow$ CALCULATEOBJETIVE($\overline{\mathbf{x}}$)
  $UB \leftarrow \min(UB, \mathcal{Z})$
  $\mu_\lambda^{(k+1)} \leftarrow$ UPDATEMULTIPLIER($\mathbf{z}^{r*}$)
  $k \leftarrow k+1$
  $gap \leftarrow (UB - LB)/UB$
end while

VI. FIC-INCORPORATED PLANNING MODELS

This section defines two mappings: $\mathbf{f}^r$ and $\mathbf{F}$, by implementing the same MILP-FIC model developed in Section IV, but with distinct outputs: $\mathcal{Z}^{r*}$ and $\mathcal{Z}^*$, respectively. Here, $\mathbf{f}^r$ and $\mathbf{F}$ are by-products of FIC, and we elaborate on two FIC-incorporated models (fleet replacement scheduling and charging resource allocation) used in the planning over the ZEB transition.

A. Fleet replacement scheduling (Long-term)

As the X-axis value and corresponding Y-axis value of route-based FIC is N^r and $\mathcal{Z}^{r*} - N^r$, respectively, define $\mathbf{f}^r : N^r \mapsto \text{FIC}(N^r) + N^r$, called fleet procurement curve (see application details in Section VIII-C1). Consider the time dimension in the replacement schedule. Let $\{0, 1, \ldots, \mathcal{H}\}$ denote a sequence of time points using a year-unit, which is indexed by a. $\mathcal{H}$ is the maximum target period to replace all current DBs, and the fleet replacement starts during year 1. Given the route-based FIC, the following model is formulated specifically for route $r \in R$, which is provided to determine the replacement schedule over the years.

$$\min_{\Delta_a^r} \sum_{a\in\{1,2,\ldots\mathcal{H}\}} K_a^r p_a - \Delta_a^r b_a \tag{18}$$

s.t.

$$I_{a+1}^r = I_a^r + \Delta_{a+1}^r \quad \forall a \in \{0, 1, \ldots, \mathcal{H}-1\}, \tag{19}$$

$$K_{a+1}^r = \mathbf{f}^r(I_{a+1}^r) - \mathbf{f}^r(I_a^r) \quad \forall a \in \{0, 1, \ldots, \mathcal{H}-1\}, \tag{20}$$

$$\underline{B}^r \le \Delta_a^r \le \overline{B}^r \quad \forall a \in \{1, 2, \ldots, \mathcal{H}\}, \tag{21}$$

$$\sum_{a\in\{1,2,\ldots\mathcal{H}\}} \Delta_a^r = M^r, \tag{22}$$

$$I_0^r = 0. \tag{23}$$

The financial burden should be minimized for BEB adoption [4], [8]. The objective of this model involves the total BEB purchasing cost and DB recycling reward. Considering the market volatility over the ZEB transition, p_a and b_a are given predictive values, denoting the unit BEB purchase price and DB salvage value during the ath year. K_a^r and Δ_a^r represent the purchasing BEB fleet and replaced DB fleet during the ath year, respectively. Constraint (19) states the update of the cumulative number of replaced DB fleet (i.e., I_{a+1}^r) during the $a+1$th year for route r. Suppose that the cumulative replaced DB fleet is I_a^r until the ath year, if additional Δ_{a+1}^r DBs will be replaced during the $a+1$th year, K_{a+1}^r can be calculated by Constraint (20). Over the ZEB transition, bus operators should manage their assets for replacing DBs of route r. To balance their budget per year, Constraint (21) enforces a bound to restrict Δ_a^r. Constraint (22) ensures all M^r DBs are replaced within the replacement period. Constraint (23) gives the initial condition.

B. Charging resource allocation

Charging resource allocation refers to the determination of siting and sizing for charging stations [22]. Since all the bus routes in R share a centralized charging site, we use mapping $\mathbf{F}$ to output the total purchasing BEB fleet. Unlike the fleet replacement schedule, the time dimension is not incorporated in this planning. Given the current state of the replaced DB fleet: $\mathcal{N} = \{N^r | \forall r \in R\}$. This subsection focuses on selecting an optimal charging resource allocation among all candidate options, based on their sitting and sizing.

Let $\mathcal{U}$ collect the candidate charging resource options, and w_u is defined as a binary variable to represent whether $u \in \mathcal{U}$ is selected. According to the sitting and sizing of

candidate locations, the attribute of option u is identified as $\mathcal{A}_u = (e_u^r, t_u^r, C_u)$, where the first two elements represent the deadheading information (energy use and time use) between the terminal of route r and location of option u, and C_u is the number of chargers deployed for option u. The model is developed as follows:

$$\min_{w_u} \sum_{u\in\mathcal{U}} w_u(c_u + \mathcal{Z}_u^* p) \tag{24}$$

s.t.

$$\sum_{u\in\mathcal{U}} w_u = 1, \tag{25}$$

$$\mathcal{Z}_u^* = \mathbf{Q}_u(\mathcal{N}) \quad \forall u \in \mathcal{U}. \tag{26}$$

The objective involves the cost of building charging sites and purchasing BEBs, whose building cost for site u corresponds to c_u, and the unit BEB purchasing cost is fixed as p, respectively. Constraint (25) states that exactly one optimal charging resource option is selected from $\mathcal{U}$, for supporting a specified replacement ratio ($\mathcal{N}$) during the ZEB transition. For option u, $\mathbf{Q}_u$ in (26) indicates an optimization over feasible region $\mathcal{S}_u$ as follows, where $\mathcal{S}_u$ is obtained by substituting parameters (e^r, t^r, C) in the constraints of the MILP-FIC as (e_u^r, t_u^r, C_u).

$$\mathbf{Q}_u(\mathcal{N}) = \min_{x_{ij}^{r,v}, z_{ij}^r \in \mathcal{S}_u} \left\{ \sum_{r\in R} \sum_{i:(o,i)\in\Omega^r} x_{oi}^{r,\mathbf{e}} \right\}. \tag{27}$$

Consequently, $\mathbf{F}^u : \mathcal{A}_u \mapsto \mathbf{Q}_u(\mathcal{N})$, and Constraint (26) is replaced as: $\mathcal{Z}_u^* = \mathbf{F}^u(\mathcal{A}_u)$. To facilitate the FIC-incorporated implementation, we first derive FICs across all candidate sites (one attribute is considered to be variant). By fixing $\mathcal{N}$, the total BEB increment can then be obtained by aggregating the FICs of R. After that, mapping $\mathbf{F}$ can be graphically represented as a curve reflecting the relationship between total BEB increment and a charging option attribute (see application details in Section VIII-C2).

Remark 2: Indeed, both $\mathbf{f}^r$ and $\mathbf{F}^u$ can be expressed as piecewise linear functions (see more details in Section VIII). Specifically for $\mathbf{f}^r$, which is characterized by a series of breaking points: $\{(b_n, \mathbf{f}^r(b_n)) | n \in \{0, 1, \ldots, A\}\}$, allowing $\mathbf{f}^r(I_a^r)$ in Constraint (20) can be computed by implementing the following linear constraints.

$$\mathbf{f}^r(I_a^r) = \sum_n \gamma_n \mathbf{f}^r(b_n), \tag{28}$$

$$I_a^r = \sum_n \gamma_n b_n, \tag{29}$$

$$\sum_n \gamma_n = 1, \tag{30}$$

$$\gamma_n \le y_n + y_{n-1}, \tag{31}$$

$$y_0 = y_A = 0, \tag{32}$$

$$\sum_n y_n = 1, \tag{33}$$

$$\gamma_n \ge 0, y_n \in \{0, 1\}. \tag{34}$$

γ_n and y_n are auxiliary variables related to breaking points b_n and the associated intervals $b_n \sim b_{n+1}$. y_0 and y_A have no physical implications and let them be zeros (see Constraint (32)). Constraints (29) and (30) are convex combination constraints of breaking points b_n. Constraint (31) enforces r_n and r_{n+1} to be non-zeros if $y_n = 1$. Constraint (33) ensures only one interval is activated. After that, two extended models can be efficiently linearized while obtaining exact planning decisions.

VII. Extension of multiple BEB types in fleet replacement scheduling

With advancements in battery technology, bus managers can have more options for a variety of BEB types featuring different battery capacities and charging powers. Our original methodology addressing a single BEB type can be further generalized to accommodate these evolving needs, and this section illustrates the extension process. Let $\{\mathbf{d}, \mathbf{e}\}$ (indexed by v) and $\mathbf{e} = \{1, 2, \ldots, L\}$ (indexed by l) denote the vehicle type set and BEB type set, respectively.

First, variables Q_i^r, $\overline{Q}_i^r$, and z_{ij}^r are replaced by $Q_i^{r,l}$, $\overline{Q}_i^{r,l}$, and $z_{ij}^{r,l}$, respectively, specifically for BEB type $l \in \mathbf{e}$. Likewise, the battery capacity D and charging profile $\Phi(\cdot)$ are also type-specific, which are replaced by D^l and $\Phi^l(\cdot)$, respectively. As different BEB types have different charging powers, causing different charging durations from 0-100% SOC, which is used to approximate $\Phi^l(\cdot)$ based on [20].

Second, Constraints (4) – (8) should be implemented in a type-specific manner. For example, Constraint (4) is modified as:

$$x_{ij}^{r,l} \ge z_{ij}^{r,l} \quad \forall l \in \mathbf{e}\ \forall r \in R\ \forall (i,j) \in \Omega^r. \tag{35}$$

Additionally, Constraints (9), (10), and (12) are modified by taking an aggregation of BEB type $l \in \mathbf{e}$. For example, Constraint (9) is rewritten as:

$$\sum_{l\in\mathbf{e}} \sum_{j:(i,j)\in\Omega^r} x_{ij}^{r,l}(Q_i^{r,l} - e^r - 0.2D^l) \ge 0 \quad \forall r \in R\ \forall i \in \mathcal{T}_r. \tag{36}$$

Third, the objective of the MILP-FIC model is modified as:

$$\min_{x_{ij}^{r,v}, z_{ij}^{r,l} \in \{0,1\}} \mathcal{Z} = \sum_{l\in\mathbf{e}} \sum_{r\in R} \sum_{i:(o,i)\in\Omega^r} \alpha^l x_{oi}^{r,l}. \tag{37}$$

Since the purchasing cost varies with different BEB types (p_a^l is defined as the purchasing cost for BEB type l in the ath year), minimizing the total fleet is not aligned with the objective in the original fleet replacement scheduling model. Assuming the purchasing costs of BEBs are dominantly affected by the battery pack costs, the variation of p_a^l is reflected by that of unit battery pack costs (measured in \$/kWh), resulting in stable relative differences between types over time. Therefore, α^l is represented as the relative difference of purchasing BEB type l compared to a baseline type.

As all the constraints except for the modified *Charging-accessibility constraint* are still route-specific, the solving approach in Section V is also applicable, while obtaining $\mathcal{Z}^{r,l*} = \sum_{i:(o,i)\in\Omega^r} \overline{x}_{oi}^{r,l}$, resulting in mapping $\mathbf{f}^{r,l} : N^r \mapsto \mathcal{Z}^{r,l*}$.

Similar to the modifications on the MILP-FIC model, the intermediate variable K_a^r further includes index l: $K_a^{r,l}$. Constraint (20) is modified to:

$$K_{a+1}^{r,l} = \mathbf{f}^{r,l}(I_{a+1}^r) - \mathbf{f}^{r,l}(I_a^r) \quad \forall l \in \mathbf{e}\ \forall a \in \{0, 1, \ldots, \mathcal{H}-1\}. \tag{38}$$

Notably, $K_a^{r,l}$ might be negative. Suppose we have two BEB types $\mathbf{e} = \{1, 2\}$. If we replace 1 DB for route r in the first year, the optimal decisions are $\mathcal{Z}^{r,1*}, \mathcal{Z}^{r,2*} = 1, 0$, but the optimal decisions might be $\mathcal{Z}^{r,1*}, \mathcal{Z}^{r,2*} = 0, 2$ when 2 DBs are replaced in the second year. As a result, $K_2^{r,1} = 0 - 1$, which is unreasonable, as the BEB type 1 purchasing in the first type can still be reused for the second year. Therefore, the following constraint should be added:

$$K_a^{r,l} \geq 0 \quad \forall l \in \mathbf{e}\ \forall a \in \{1, 2, \ldots, \mathcal{H}\}. \tag{39}$$

Objective (18) in the fleet replacement scheduling model is updated to:

$$\min_{\Delta_a^r} \sum_{l \in \mathbf{e}} \sum_{a \in \{1,2,\ldots\mathcal{H}\}} K_a^{r,l} p_a^l - \Delta_a^r b_a. \tag{40}$$

VIII. Numerical Experiments

We investigate the FIC and two of its applications within the Hong Kong bus network. Traditional double-decker DBs are replaced with double-decker BEBs, each featuring a 472-kWh battery [23] which requires almost two hours [6] to get fully charged from 0% to 100%. Based on the real charging track from [20], vehicles are charged in the linear segment of the charging curve ending at roughly 80% of the capacity, while the remaining profile after reaching 80% is approximated as a piecewise linear function. This prior work suggested three phases from 0% to 100%, and the original charging profile is given as:

$$\hat{\Phi}(t) = \begin{cases} 302.08t & t \in [0, 1.25] \\ 377.6 + 188.8(t - 1.25) & t \in (1.25, 1.5] \\ 424.8 + 94.4(t - 1.5) & t \in (1.5, 2] \end{cases}$$

The variable t represents time in hours. This function reflects the variation of remaining energy with charging duration, characterized by a charging rate that decreases across its three phases. By extending the maximum charging duration of $\hat{\Phi}(t)$ (> 2 hours), we can derive function $\Phi(t)$ following Remark 1. Our analysis begins by examining how route characteristics (Section VIII-A) and charging site characteristics (Section VIII-B) influence the FIC configuration. Subsequently, we evaluate the outcomes of two FIC-integrated applications (fleet replacement scheduling and charging resource allocation) in Section VIII-C.

A. Impact of route characteristics on FIC

As aforementioned, a charging site provides centralized charging service for bus routes in R, including eight bus routes (operated by the KMB bus company) with terminals in close proximity (shown in Figure 3). Table III highlights the route characteristics, including # of round trips, route service duration, and route energy use.

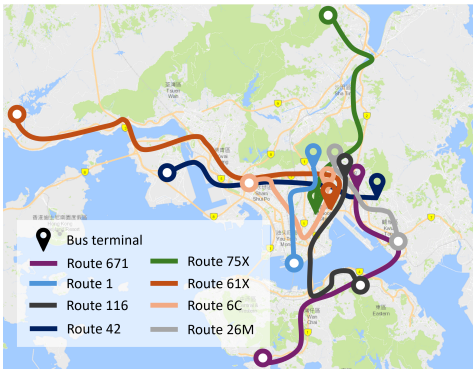

Fig. 3. Sketch map of eight bus routes in Hong Kong

TABLE III
Characteristics of Bus Routes

Route ID	# of round trips	T^r (min)	E^r/D
671	32	180	40.05%
1	87	130	13.73%
116	85	176	24.90%
42	48	168	29.03%
75X	66	196	38.70%
61X	58	164	53.70%
6C	81	136	15.30%
26M	47	142	18.45%

The analysis in this subsection assumes no limit on charging accessibility. Based on the total DB fleet size (M^r) before the ZEB transition, Figure 4 records the variation BEB increment needed for replacing different # of DBs (from 0 to M^r, with a 1-unit increment).

The overall results show that the routes, except for Route 116 (1:1 replacement is feasible), require BEB fleet expansion beyond their original total DB fleet M^r until the achievement of the ZEB system. That is, purchasing the same number of DB fleet might not maintain the trip services of most bus routes, which stems from the limited driving range and prolonged charging duration of BEBs. Additionally, several routes exhibit S-shaped FICs, where zero BEB increment is required initially, and it remains a stable final phase when approaching full electrification.

The results highlight the impact of route characteristics (e.g., trip frequency, total traveling duration, and energy use of bus routes) on the FIC. A notable comparison between Route 1 and Route 116 (with similar number of trips) shows that despite the higher energy consumption for Route 116, it requires no additional BEBs to replace its DB fleet. This observation results from the longer route service duration (T^r) for Route 116, which necessitates more fleet in rotation, ultimately reducing average serving trip counts of each bus and its total energy use.

Among high-energy routes (671, 75X, and 61X), Route 61X requires the largest BEB increment mainly because of its highest E^r. Interestingly, no BEB increment is needed until exceeding 9 replaced DBs. The potential reason is the underutilized DBs for serving trips (same original DB fleet as

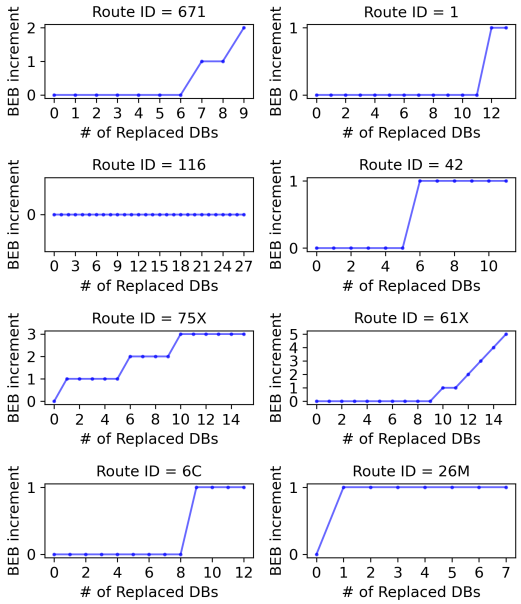

Fig. 4. FIC of different routes

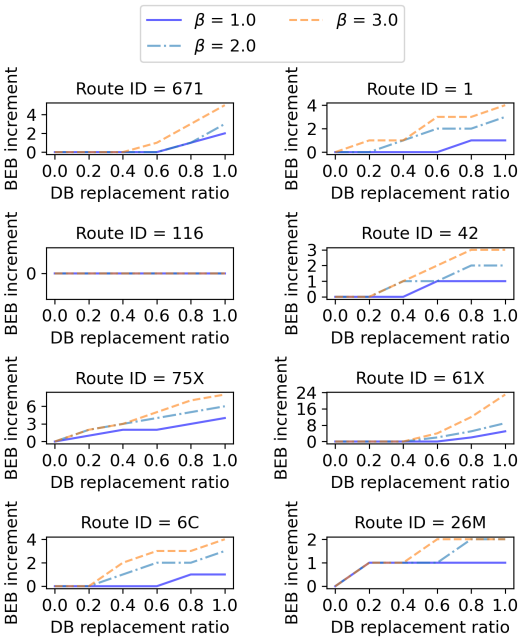

Fig. 5. Impact of different charging site sitings (specified by β) on FIC.

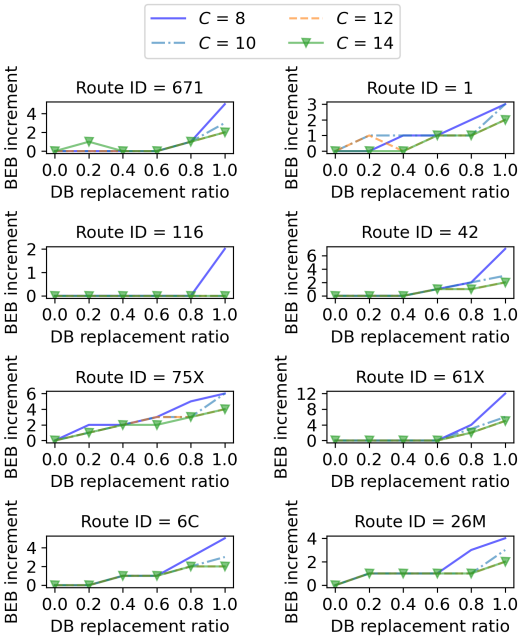

Fig. 6. Impact of different charging site sizes (specified by C) on FIC.

Route 75X but with less trip frequency). These idle DBs can compensate for the trips that cannot be served by BEBs due to their limited driving range. Even if Route 671 needs more energy use compared to Route 75X, the lower trip frequency leads to fewer trips to be served. Besides, the lower trip frequency leads to longer layover duration, providing more opportunity for BEB charging. Therefore, the BEB increment of Route 671 is lower than that of Route 75X.

B. Impact of charging site characteristics on FIC

To analyze the impact of charging site characteristics, we incorporate various feasible regions into the optimization model (27) using different charging site information. We also consider eight routes from Table III. The *DB replacement ratio* (θ), represents the ratio of the number of replaced DBs to the original DB fleet size, satisfying $N^r = \lceil M^r * \theta \rceil$ for all routes. Consequently, the same θ ranging from 0.0 to 1.0 with a 0.2 increment is applied across all routes.

1) Impact of siting of the charging site: The placement of the charging site affects both the duration of potential charging events (W_{ij}^r), which changes with t_r, and e_r. For simplicity, a default siting: $t_r, e_r = 10$ min, 10 kWh, respectively, is assumed for each route r. To represent different site locations, we define a scaling factor β to multiply the default values.

The findings in Figure 5 reveal that when β increases, the FIC generally rises across all routes, except for Route 116, which exhibits lower fleet utilization. A higher β indicates a more distant charging site, resulting in more time spent on conducting charging events, and more BEB fleets are required for maintaining trip services. In particular, the BEB increment of Route 61X dramatically increases as β increases. For Route 26M, while it ultimately (when $\theta = 1.0$) requires the same number of BEBs for $\beta = 2.0$ and $\beta = 3.0$, where a more distant charging site (higher β) leads to an earlier BEB procurement to maintain the trip service.

2) Impact of sizing of the charging site: The sizing of the charging site is specified as the number of available chargers (C). As in previous analyses, we apply the same replacement ratio range to assess the FIC. Unlike the results in Figure 5, where FIC is consistently plotted higher with larger β, the results in Figure 6 fail to show this consistent phenomenon with fewer chargers (lower C). For example, Route 671

requires one BEB increment when $\theta = 0.2$ and $C = 14$, compared to that when $C = 8$. In the meantime, Route 75X requires one additional BEB increment when $C = 8$. This observation arises because the centralized charging site must coordinate charging events across multiple routes. Notably, when $\theta \leq 0.6$, the total BEB increment of all the routes a slightly changes regardless of C values. For comparison, a significant difference in the BEB increment for all routes happens when θ is larger than 0.6. This observation reveals that the charging site sizing significantly impacts FIC shape when more DB fleets are replaced. Unlike the impact of charging site siting, where a more distant charging site leads to a non-decreasing BEB increment across all routes, the limited charger provision enables the coordination of charging events (e.g., adjusting their charging amount and charging periods) across all routes to maintain a stable BEB adoption. This suggests that, particularly at lower DB replacement ratios, strategic charger placement is more critical than expanding capacity in minimizing additional BEB adoption.

C. FIC-incorporated applications

The following subsections focus on FIC-incorporated two applications: i) fleet replacement schedule; and ii) charging resource allocation, which have been described in Section VI. In this context, we present associated planning decisions using the FIC outputs.

1) Fleet replacement scheduling: We use Route 75X as an example. Based on the FIC output of Route 75X in Figure 4, $\mathbf{f}^r(.)$ can be mathematically obtained as:

$$\mathbf{f}^r(.) = \begin{cases} 0 & N = 0, \\ N+1 & 0 < N \leq 5, \\ N+2 & 5 < N \leq 9, \\ N+3 & 9 < N \leq 15, \end{cases}$$

This piecewise linear function results in breaking points: (0, 0), (0, 1), (5, 6), (5, 7), (9, 11), (9, 12), (15, 18). The ZEB system requires that all the DBs serving this route be replaced by 2035, while initiating the replacement in 2025. In Section VI-A, the unit BEB purchase cost and DB salvage value are denoted p_a and b_a, and both of them vary with years. Referred to [4], [8], [9], p_a is supposed to follow a decreasing trend due to advancements of battery technology, while b_a declines with vehicle aging. This reduction is captured by the exponential equations: $p_a = p_0(1+\zeta_1)^{-a}$ and $b_a = b_0(1+\zeta_2)^{-a}$, where ζ_1 and ζ_2 represent the discount rate of purchase cost and salvage value, respectively. Based on the latest market data in [24], the initial purchase cost $p_0 = 3.6$ million HK$ for a double-deacker BEB and 2.8 million HK$ for a double-decker DB. According to the residual value percentage reported in [25], the salvage value of DBs is approximated as $b_0 = 0.8$ million HK$. Figure 7 provides the variation details of p_a and b_a from 2025 to 2035 by implementing different discount rates. To reflect the global ambition for the ZEB transition, we apply a higher discount rate to b_a, as evidence suggests they are depreciating more rapidly than p_a [1].

From the results given in Figure 4, the total of 15 DBs should be replaced during the ZEB transition for Route 75X. Figure 8 presents six replacement scheduling resulting from varying combinations of cost and reward deductions. To balance the annual budget, the number of replaced DBs is uniformly bounded within $1 \sim 4$ for each year. It is found that when ζ_1 equals 0.04, it would be better to delay the DB replacement, as early BEB adoption incurs higher purchasing costs, even with a larger discount rate ζ_2 for DB salvage value. When the cost is not significantly reduced (ζ_1 equals 0.02), the value of ζ_2 for DB salvage becomes the decisive factor in determining the replacement schedule, where a significant reduction of DB salvage value (higher ζ_2) incentivizes early DB replacement over the ZEB transition.

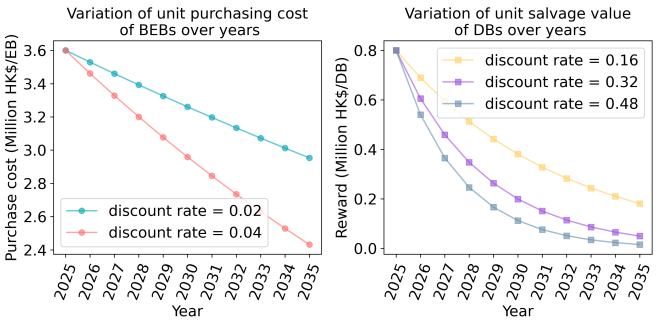

Fig. 7. Variation of BEB purchase cost and DB salvage value with different discount rates (from 2025 to 2035).

Fig. 8. Fleet replacement schedule with different purchase discount rates and salvage discount rates (the original DB fleet before ZEB transition is 15).

2) Charging resource allocation: The results in Figure 6 reveal the relationship between BEB fleet expansion and the number of chargers (C) at different replacement ratios. Based on the model provided in Section VI-B, we replace c_u with the installation costs of chargers. For instance, $c_u = C_u * \sigma$ for representing different charging site sizing, where σ is the unit cost of installing chargers. If the land use costs are not considered, σ is much cheaper than the BEB purchasing price. Hereby, this simplified scenario helps determine the minimum number of chargers needed to minimize the total BEB fleet expansion. Herein, we assume the charging site can maximally accommodate 14 chargers.

Figure 9 provides the variation of total BEB increment (all routes) with different charging site sizes. It is observed that deploying more chargers cannot always lead to a decrease in BEB increment. With a higher DB replacement ratio, more BEBs will be introduced with the same number of chargers. Additionally, the comparative results reveal that a higher replacement ratio leads to a more sensitive reduction of total BEB increment. From the results, we can easily get

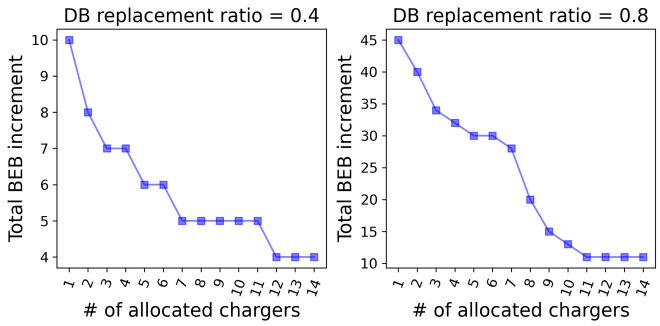

Fig. 9. The varying total BEB increment of all the routes with different charging site sizes.

the optimal charging site with optimal $C = 12$ and 11 when the DB replacement ratio equals 0.4 and 0.8, respectively. This result provides a counterintuitive insight: given the maximum number of chargers allowed to be deployed, the optimal number of allocated chargers will not increase for a scenario with more DBs to be replaced.

IX. Conclusions

The transition to ZEB through the replacement of DBs with BEBs mostly requires a larger fleet size than the original DB fleet. Using the information on this increment with different replaced DB fleets, this study introduces the concept of the Fleet Increment Curve (FIC), enabling bus operators to make strategic decisions and retrofit their infrastructures. We first develop an MILP-FIC model to derive the FIC, and an LR approach is applied to solve this model, with optimal solutions informing the FIC configuration. By representing FIC by-products as piecewise linear functions, we develop two extended models incorporating FIC into the fleet replacement schedule and charging resource allocation. To keep pace with advancements in battery technology, the developed methodology is extended to support BFR decisions for multiple BEB types.

The methodology is tested within the Hong Kong bus network, and our analysis reveals the impact of route and charging site characteristics on FICs. Specifically, the stable curve indicates that underutilized buses potentially eliminate the need for purchasing additional BEBs. The results underscore the importance of deploying sufficient chargers in strategic, nearby locations (around terminals) during the ZEB transition. At lower DB replacement levels, constrained charging site capacity results in FIC coordination across routes to maintain a steady BEB adoption.

Two FIC-incorporated models are verified by obtaining the fleet replacement scheduling and determining the optimal charger deployment strategy. Comparative analysis reveals the impact of market variation on the fleet replacement scheduling, where a lower discount rate for BEB purchase costs (0.02) combined with a higher discount rate for the DB salvage value (0.48) creates an incentive for a larger initial replacement scale. When the DB replacement ratio reaches a higher level, allocating more chargers within a certain range leads to a more sensitive decline in BEB increment. A counter-intuitive finding for the 8-route case is that doubling the DB replacement rate (from 0.4 to 0.8) reduces the number of chargers required to achieve the minimum BEB fleet by 1. More broadly, the results indicate that beyond a certain point, adding more chargers does not alter the BEB increment, informing bus operators that excessive charger deployment may not always be beneficial for decreasing BEB adoption.

As an intermediate work, future research directions include investigating the joint impact of the schedule of replacing DBs and building charging sites. Additionally, further investigation is warranted into the potential of treating battery capacity and charging power as design variables during the ZEB transition.

References

[1] International Energy Agency, *Global EV outlook 2025*, 2025. [Online]. Available: https://www.iea.org/reports/global-ev-outlook-2025.

[2] Shenzhen Bus Report, *Electrification of Public Transport: A Case Study of the Shenzhen Bus Group*, 2021. [Online]. Available: https://documents1.worldbank.org/curated/en/708531625052490238/pdf/Electrification-of-Public-Transport-A-Case-Study-of-the-Shenzhen-Bus-Group.pdf.

[3] L. Li, H. K. Lo, and X. Cen, "Optimal bus fleet management strategy for emissions reduction," *Transportation Research Part D: Transport and Environment*, vol. 41, pp. 330–347, 2015.

[4] A. Islam and N. Lownes, "When to go electric? A parallel bus fleet replacement study," *Transportation Research Part D: Transport and Environment*, vol. 72, pp. 299–311, 2019.

[5] Z. Ye, Z. Huang, S. Yang, Y. Du, and H. Zhao, "Electric bus fleet transition: Assessment approach considering economic and environmental impacts, and its application," *Smart Construction and Sustainable Cities*, vol. 2, no. 1, p. 17, 2024.

[6] South China Morning Post, *Future is electric for Hong Kong's bus fleet, says world's biggest manufacturer Alexander Dennis*, 2024. [Online]. Available: https://www.scmp.com/business/companies/article/3262822/future-electric-hong-kongs-bus-fleet-says-worlds-biggest-manufacturer-alexander-dennis.

[7] S. Pelletier, O. Jabali, J. E. Mendoza, and G. Laporte, "The electric bus fleet transition problem," *Transportation Research Part C: Emerging Technologies*, vol. 109, pp. 174–193, 2019.

[8] M. T. Navarrete, J. S. Reyes, J. V. Godiño, and F. J.-E. Aguilar, "Clean and zero-emission urban buses: Compliance with EU regulations and fleet transition in Seville," *Energy*, p. 137 025, 2025.

[9] A. Avenali, D. De Santis, M. Giagnorio, and G. Matteucci, "Bus fleet decarbonization under macroeconomic and technological uncertainties: A real options approach to support decision-making," *Transportation Research Part E: Logistics and Transportation Review*, vol. 190, p. 103 690, 2024.

[10] Y. Zhou, G. P. Ong, and Q. Meng, "The road to electrification: Bus fleet replacement strategies," *Applied Energy*, vol. 337, p. 120 903, 2023.

[11] Y. Zhou, X. C. Liu, R. Wei, and A. Golub, "Bi-objective optimization for battery electric bus deployment considering cost and environmental equity," *IEEE Transactions on Intelligent Transportation Systems*, vol. 22, no. 4, pp. 2487–2497, 2020.

[12] T. Lu, E. Yao, Y. Zhang, and Y. Yang, "Joint optimal scheduling for a mixed bus fleet under micro driving conditions," *IEEE Transactions on Intelligent Transportation Systems*, vol. 22, no. 4, pp. 2464–2475, 2021.

[13] Ş. Yıldırım and B. Yıldız, "Electric bus fleet composition and scheduling," *Transportation Research Part C: Emerging Technologies*, vol. 129, p. 103 197, 2021.

[14] Y. Cong, Y. Bie, Z. Liu, and A. Zhu, "Collaborative vehicle-crew scheduling for multiple routes with a mixed fleet of electric and fuel buses," *Energy*, vol. 298, p. 131 400, 2024.

[15] M. Alvo, G. Angulo, and M. A. Klapp, "An exact solution approach for an electric bus dispatch problem," *Transportation Research Part E: Logistics and Transportation Review*, vol. 156, p. 102 528, 2021.

[16] Y. Peng, G. Li, M. Xu, and A. Chen, "Mixed-fleet operation of battery electric bus and hydrogen bus: Considering limited depot size with flexible refueling processes," *Transportation Research Part E: Logistics and Transportation Review*, vol. 188, p. 103 630, 2024.

[17] M. H. de Vos, R. N. van Lieshout, and T. Dollevoet, "Electric vehicle scheduling in public transit with capacitated charging stations," *Transportation Science*, vol. 58, no. 2, pp. 279–294, 2024.

[18] A. Shehabeldeen, A. Foda, and M. Mohamed, "A multi-stage optimization of battery electric bus transit with battery degradation," *Energy*, vol. 299, p. 131 359, 2024.

[19] Z. Cui, X. Fu, H. Jin, A. Chen, and K. Wang, "Transitioning to electrification: Optimal strategies for ship fleet replacement," *Transportation Research Part C: Emerging Technologies*, vol. 174, p. 105 079, 2025.

[20] A. Montoya, C. Guéret, J. E. Mendoza, and J. G. Villegas, "The electric vehicle routing problem with nonlinear charging function," *Transportation Research Part B: Methodological*, vol. 103, pp. 87–110, 2017.

[21] Y. Zhou, Q. Meng, and G. P. Ong, "Electric bus charging scheduling for a single public transport route considering nonlinear charging profile and battery degradation effect," *Transportation Research Part B: Methodological*, vol. 159, pp. 49–75, 2022.

[22] S. S. Barhagh, B. Mohammadi-Ivatloo, M. Abapour, and M. Shafie-Khah, "Optimal sizing and siting of electric vehicle charging stations in distribution networks with robust optimizing model," *IEEE Transactions on Intelligent Transportation Systems*, vol. 25, no. 5, pp. 4314–4325, 2023.

[23] Clean Technica, *Hong Kong's KMB gets next-generation Enviro500EV zero-emission double-decker buses*, 2023. [Online]. Available: https://cleantechnica.com/2023/05/11/hong-kongs-kmb-gets-next-generation-enviro-500-ev-zero-emission-double-decker-buses/.

[24] Civil Exchange, *A pathway for the deployment of hydrogen in Hong Kong's public buses.* 2024. [Online]. Available: https://documents1.worldbank.org/curated/en/708531625052490238/pdf/Electrification-of-Public-Transport-A-Case-Study-of-the-Shenzhen-Bus-Group.pdf.

[25] A. Smyth, E. Bigelow, M. Henderson, *et al.*, "Resilient zero-emission transit bus fleets: A guide," Tech. Rep., 2025.

Yiyang Peng received his B.S. and M.S. degrees in transportation engineering from Southwest Jiaotong University, Chengdu, China, in 2016 and 2021, respectively. He is currently pursuing a Ph.D. degree with the Department of Civil and Environmental Engineering, The Hong Kong Polytechnic University. His research interests include electrified transit operation and transportation network modeling.

Zhuowei Wang received her B.S. and M.S. degrees from Harbin Institute of Technology, Harbin, China, in 2017 and 2020, respectively. She is currently pursuing a Ph.D. degree with the Department of Civil and Environmental Engineering at The Hong Kong Polytechnic University. Her research interests include system dynamics modeling, life-cycle assessment, integrated transportation-energy systems, and policy analysis.

Anthony Chen received his Ph.D. degree from the University of California at Irvine, Irvine, CA, USA, in 1997. From 2015 to 2017, he was selected into the National High-Level Talent Program at Tongji University, Shanghai, China. He is currently a Professor and Associate Head of the Department of Civil and Environmental Engineering, The Hong Kong Polytechnic University, Hong Kong, China. The majority of his research focuses on transportation system modeling and analysis, transportation network reliability and resiliency analysis, and applied optimization to civil infrastructure problems and emerging technologies.